

Automated Blood Cell Classification Using Convolutional Neural Networks

Dr. S. Sreenath Kashyap,

Associate Professor, Dept. of ECE, Kommuri Pratap Reddy Institute of Technology, Hyderabad. sreenathkashyaps@gmail.com

M. Ramana Kumar,

Assistant Professor, Dept. of CSE, Shadan Women's College of Engineering & Technology, Hyderabad, Telangana. drmrkumar2020@rediffmail.com

Abstract

Deep Learning has developed into a significant tool across multiple applications, achieving broad acceptance compared to conventional machine learning models. The application of deep learning algorithms, specifically Convolutional Neural Networks (CNN), has markedly progressed the medical domain, where extensive quantities of images necessitate detailed processing and analysis. This document presents the development of a deep learning model aimed at addressing the intricate challenge of blood cell classification, which is a vital component of blood diagnostics. This document outlines a framework utilizing convolutional neural networks (CNN) for the automatic classification of blood cell images into designated subtypes. Extensive experiments are performed on a dataset that includes 13,000 blood cell images along with their respective subtypes. The results indicate that the proposed model outperforms existing alternatives, exhibiting enhanced performance across multiple evaluation metrics.

1. Introduction

Sickle cell disease (SCD), also known as sickle cell anemia, is a type of inherited RBC disorder associated with abnormal hemoglobin S (HbS) [1]. When HbS molecules polymerize inside RBCs, due to lack of oxygen, they affect greatly the shape, elasticity, and adhesion properties of RBCs. Moreover, the RBCs become stiff and more fragile, with vastly heterogeneous shapes in the cell population [2], which makes this problem an ideal candidate for the examination of morphological heterogeneity. Unlike the normal RBCs, which are flexible and move easily even through very small blood vessels, sickle RBCs promote vaso-occlusion phenomena. Hence, SCD patients are afflicted with the risk of life-threatening complications, stroke and organ damage over time, resulting in a reduced life expectancy. According to a recent study [3], as of 2013 about 3.2 million people have SCD while an additional 43 million have sickle cell trait, resulting in 176,000 deaths in 2013, up from 113,000 deaths in 1990, mostly of African origin. The prime hallmark of SCD is that is surprisingly variable in its clinical severity. Available methods for treating SCD are mainly supportive and mostly aim at symptom control, but lack the active monitoring of the health status as well as the prediction of disease development in different clinical stages [4]. Recent developments in advanced medical imaging technology and computerized image processing methods could provide an effective tool in monitoring the status of SCD patients. Indeed, Darrow et al. [5] recently demonstrated a positive correlation between cell volume and protrusion number using soft X-ray tomography. Van beers et al. [6] have also shown highly specific and sensitive sickle and normal erythrocyte classification based on sickle imaging flow cytometry assay, a methodology that could be useful in assessing drug efficacy in SCD. Therefore, implementing an automated, high-throughput cell classification method could become an enabling technology to improve the future clinical diagnosis, prediction of treatment outcome, and especially therapy planning. However, there are several major technical challenges for automatic cell classification: 1) RBCs may touch or overlap each other or appear as clusters in the image, which makes it difficult to detect the hidden edge of cells. 2) The RBC region and the background may have low contrast in the intensity. 3) The boundaries of RBCs may be blurry due to the influence of imaging procedure. 4) Very complex and heterogeneous shapes of RBCs are present in SCD. 5) Artifacts may be present, for instance, dirt on the imaging light path, various halos and shading. 6) Finally, because RBCs lack a nucleus, methods utilizing the nuclei location as an apparent marker for cell counting and detection are not applicable.

Keywords:

Blood cells, medical diagnosis, Deep learning, Convolutional neural networks.

Doi:

10.5455/jcmr.20190513073649

Due to ineffectiveness of the aforementioned methods and given the recent advances of deep learning technique, Gao et al. [1] performed HEp-2 cell classification based on deep CNNs. Also, in order to improve the diversity of single HEp-2 cell data samples, Li et al. [2] carried out classification experiments based on deep CNNs by using four different patients' datasets under different lighting conditions. However, for the currently available automated machine learning methods, which could be used for cell classification, the following are still drawbacks: 1) the classification studies are mostly directly based on already prepared single HEp-2 cellular data, hence, ignoring the initial key procedure of single cell extraction from the raw image data; 2) the adopted conventional machine learning methods are time consuming for the hand-crafted feature extraction and need specific human expertise; moreover, they need an accurate cell segmentation; 3) the classification accuracy is limited by the selected features and the performance of selected classifier. For our application, since RBCs of SCD exhibit special characteristics in terms of heterogeneous shapes and variant sizes, there is still no efficient tool that can be used to facilitate the automated inspection and recognition of various kinds of RBC patterns which are present in SCD blood. The main focus of our paper is to develop an automated, high-throughput sickle cell classification method based on the Convolutional Neural Networks (CNNs), taking advantage of the hierarchical feature learning goodness of deep learning.

2. Proposed method

Convolutional neural networks have shown success in image classification [23- 25]. the strength of a CNN

lies on its ability to employ a multilayer architecture to automatically extract high-level features through a series of convolutional, nonlinear transformation, downsampling (pooling), and fully connected layers of the network. To train a CNN for image classification, first the network architecture must be designed. This task is to determine the types, number, and order of layers in the network. the designed network, given a set of 2D images along with their corresponding class labels, attempts to find features useful for distinguishing the classes. A CNN employs a learning method that consists of two repeated and alternated passes, naming feedforward and backward pass. A typical CNN's feedforward pass performs two major tasks. the first task is feature extraction via the use of multiple convolutional feature extraction (CFE) layers. For this task, an image is passed through multiple CFE layers in a serial manner. A CFE layer consists of three sublayers: a convolutional sublayer, followed by a nonlinear transformation sublayer, and then by a pooling sublayer. Each CFE layer takes features from the previous layer and constructs higher-level features. This process often repeats many times in order to eventually extract high-level features from the image. These features then become input for the fully connected layers in the second task of a feedforward pass, which performs classification of the input image and obtains some error. In a backward pass, the error obtained from a feedforward pass propagates backward to adjust the weights in the convolutional sublayers, and therefore, they can better extract features relevant to the classification problem. the same error is also used to find proper weights for the fully connected layers.

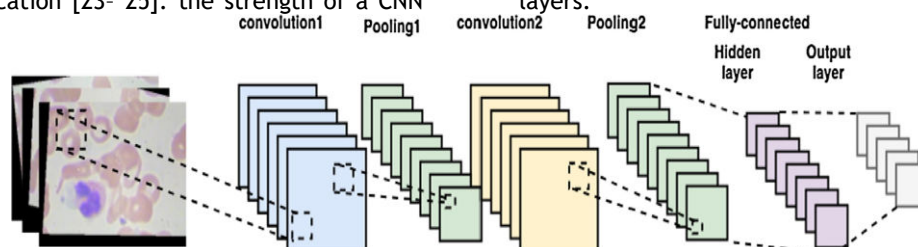


Figure 1: Architecture of ConvNet

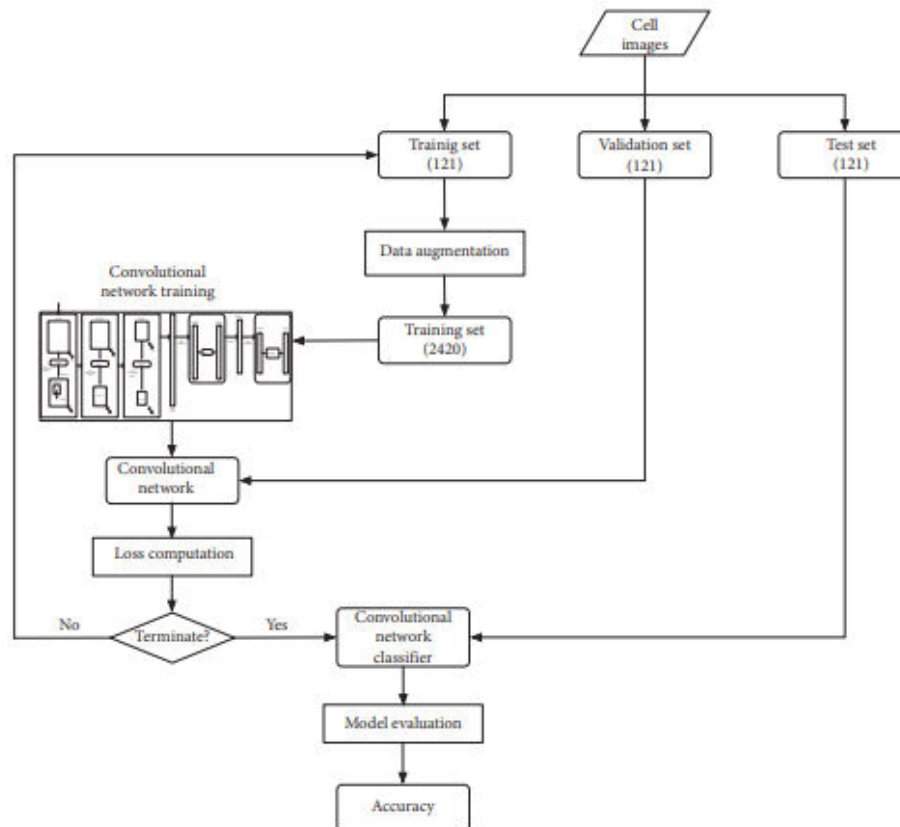


Figure 2: Image classification using ConvNet.

Architecture of ConVNet: the overall architecture of ConVNet used in this study is shown in Figure 1. The network consists of seven layers, excluding the input layer. The input layer takes in a 256×256 RGB color image when each color channel is processed separately. The first, second, and third layers of ConVNet are CFE layers. the first and second CFE layer each applies 32 of 3×3 filters to an image in the convolutional sublayer. the image's border is padded with 0 to maintain the image size of 256. The nonlinear transformation sublayer employs the ReLU activation function. the max pooling sublayer applies a 2×2 filter to the image which results in reducing the image size to its half. The third CFE layer has similar structure to the first one, except the number of filters is 64. At this point, ConVNet extracts 64 features, each represented by a 32×32 array for each color channel. The fourth layer is a flatten layer. The flatten layer transforms a multidimensional array into one-dimensional array by simply concatenating the entries of the multidimensional array together. the output of this flatten layer is a one-dimensional array of size 65536. The fifth layer is a fully connected artificial neural network (ANN) with the ReLU activation function that maps 65536 input values to 64 output values. The sixth layer is a dropout layer. 50 percent of the input values coming into this layer are dropped to zero to reduce the problem of overfitting. The seventh layer is a fully connected

ANN with the sigmoid activation function that maps 64 input values to 3 class labels. The CNN consists of seven layers. Layers 1, 2, and 3 implement feature extraction of cell images. Layer 4 transforms 64 extracted features into one-dimensional array of size 65536. Layer 5 maps 65536 inputs into 64 outputs. Layer 6 drops 50 percent of the 64 inputs at random. Layer 7 performs classification of 3 types of ALL subtypes.

Procedure of ConVNet. The overall procedure of image classification using ConVNet is presented in Figure 2. Since a large amount of data is essential in achieving high performance for CNN, we utilize data augmentation techniques to increase the number of images in the training set from 121 to 2420 images. the operations used for data augmentation are horizontal flip, shearing within 0.2 radians in the counterclockwise direction and zooming between 0.8 and 1.2. First, we train ConVNet using the data in training set to find appropriated filters' weights in the three convolutional sublayers and the weights that yield minimum error in the two fully connected layers. Next, we evaluate ConVNet using the data in the validation set to obtain validation error and cross-entropy loss. We then train ConVNet again using a new training set created from data augmentation of the original 121 training images. We repeat the training of ConVNet in this same procedure until we complete 50 epochs. Last, we

evaluate the performance of ConVNet using data in the test set.

3. Results and discussion

To evaluate the performance of our deep learning approach, we compare ConVNet with the dominant approach of SVM-GA and two traditional machine learning methods, namely, MLP and random forest. Table 5 depicts the accuracy results obtained from these approaches taking ten test sets and shows the average with standard deviation over the ten

performance estimates. Considering the average accuracy, the two traditional approaches cannot achieve the accuracy above 80% while ConVNet and SVM-GA yield the average accuracy above 80% and produce comparable results with the deference on a very small margin. From the ten set runs, most of the results obtained by both ConVNet and SVM-GA are above 80% and have the number approximately ranging from 78-86%.



Fig 3: detection of blood cell

```
In [16]: if result[0] == 0:
...:     prediction = 'EOSINOPHIL'
...: elif result[0] == 1:
...:     prediction = 'LYMPHOCYTE'
...: elif result[0] == 2:
...:     prediction = 'MONOCYTE'
...: elif result[0] == 3:
...:     prediction = 'NEUTROPHIL'
...:
...:
...: print('Actual picture is : LYMPHOCYTE')
...: print('Model prediction is : ',prediction)
Actual picture is : LYMPHOCYTE
Model prediction is : LYMPHOCYTE
```

Fig 4: classification of blood cell

Layer (type)	Output Shape	Param #
conv2d_1 (Conv2D)	(None, 62, 62, 32)	896
max_pooling2d_1 (MaxPooling2D)	(None, 31, 31, 32)	0
conv2d_2 (Conv2D)	(None, 29, 29, 32)	9248
max_pooling2d_2 (MaxPooling2D)	(None, 14, 14, 32)	0
flatten_1 (Flatten)	(None, 6272)	0
dense_1 (Dense)	(None, 128)	802944
dense_2 (Dense)	(None, 4)	516
Total params: 813,604		
Trainable params: 813,604		
Non-trainable params: 0		

Fig 5: neural network analysis

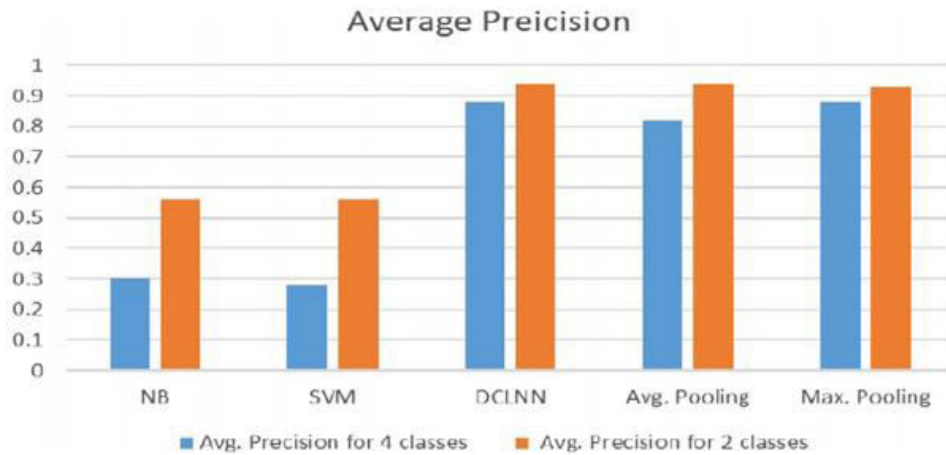


Fig. 6. Average Precision comparison

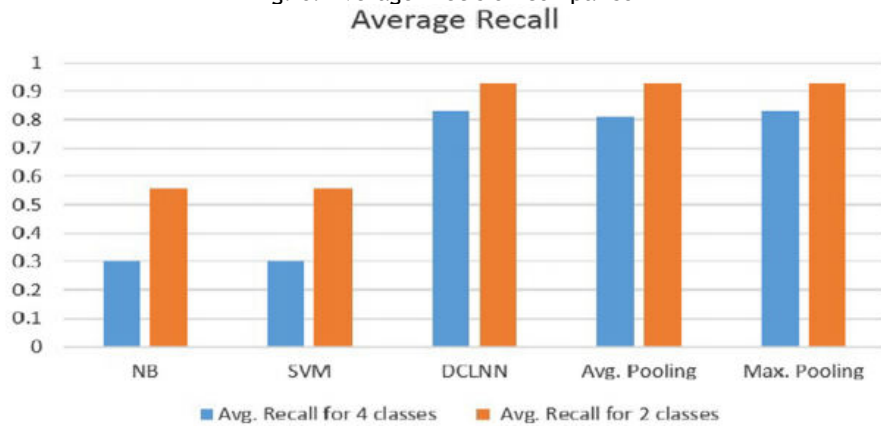


Fig. 7. Average Recall comparison

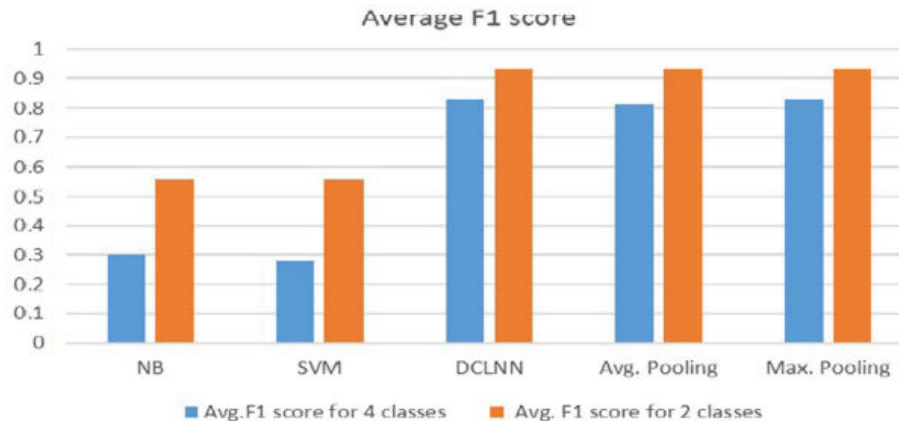


Fig. 8. Average F1 score comparison

Moreover, We conduct another series of experiments, with the attempt to determine the technique for the pooling layer: MaxPooling and AveragePooling. For four classes, AveragePooling has better performance at some points, e.g., precision of neutrophil classifier, recall of the eosinophil classifier, etc. However, comprehensively MaxPooling outperforms AveragePooling. The average performance (precision, recall and F1 score) is graphically demonstrated in Figs. 4-6. Referring to two classes, they are virtually identical. Last but not least, to determine the optimal number of epochs for training and validation we exhaustively iterate variant number and compute the precision, in Fig. 7. The red line indicates the training precision and the blue line is the validation precision. We conclude that 25 is a good option trade-off between precision and computing time. Our proposed model outperform the traditional machine learning models which can be very useful in the medical field and this proposed model allow to get rid from the blood diagnosis problems.

4. Conclusion

From the obtained experiments, Our proposed models suggest that implementation of deep learning enhance the classification task as compared to state-of-art models. SVM and Naive Bayes has been utilized as a baseline to compare with the proposed CNN based model and it compete in all aspects with the baseline approaches. Our proposed model can automatically classify the blood cell images into subtypes of the cells with high accuracy, precision and other evaluation parameters. This proposed model can be very beneficial for blood diagnosis in the medical field that can save a lot of time. We believe that there is always room for improvement in every field so as well in this field also. Researchers may implement this work on large dataset that may outperform the current results

References

- [1] Jordan, M. I. & Mitchell, T. M. Machine learning: Trends, perspectives, and prospects. *Science* 349, 255-260, doi:10.1126/science.aaa8415 (2015).
- [2] van Ginneken, B. Fifty years of computer analysis in chest imaging: rule-based, machine learning, deep learning. *Radiological Physics and Technology* 10, 23-32, doi:10.1007/s12194-017-0394-5 (2017).
- [3] de Bruijne, M. in *Med Image Anal Vol. 33* 94-97 (Elsevier, 2016).
- [4] Kerr, W. T., Lau, E. P., Owens, G. E. & Trefler, A. The future of medical diagnostics: large digitized databases. *Yale J Biol Med* 85, 363-377 (2012).
- [5] Kukar, M., Kononenko, I. & Grošelj, C. Modern parameterization and explanation techniques in diagnostic decision support system: A case study in diagnostics of coronary artery disease. *Artificial intelligence in medicine* 52, 77-90 (2011).
- [6] Šajn, L. & Kukar, M. Image processing and machine learning for fully automated probabilistic evaluation of medical images. *Computer methods and programs in biomedicine* 104, e75--e86 (2011).
- [7] Esteva, A. et al. Dermatologist-level classification of skin cancer with deep neural networks. *Nature* 542, 115-118, doi:10.1038/nature21056 (2017).
- [8] Yamamoto, Y. et al. Quantitative diagnosis of breast tumors by morphometric classification of microenvironmental myoepithelial cells using a machine learning approach. *Scientific Reports* 7, 46732, doi:10.1038/srep46732 (2017).
- [9] Badrick, T. Evidence-based laboratory medicine. *The Clinical Biochemist Reviews* 34, 43 (2013).
- [10] Luo, Y., Szolovits, P., Dighe, A. S. & Baron, J. M. Using Machine Learning to Predict Laboratory Test Results. *American journal of clinical pathology* 145, 778-788, doi:10.1093/ajcp/aqw064 (2016).